A&A 549, A113 (2013)
DOI: 10.1051/0004-6361/201220272

Astronomy & Astrophysics

Torsional Alfvén waves in partially ionized solar plasma: effects of neutral helium and stratification

T. V. Zaqarashvili[1,3], M. L. Khodachenko[1], and R. Soler[2]

[1] Space Research Institute, Austrian Academy of Sciences, Schmiedlstrasse 6, 8042 Graz, Austria
e-mail: [teimuraz.zaqarashvili;maxim.khodachenko]@oeaw.ac.at
[2] Departament de Física, Universitat de les Illes Balears, 07122 Palma de Mallorca, Spain
e-mail: roberto.soler@uib.es
[3] Abastumani Astrophysical Observatory at Ilia State University, University St. 2, 1060 Tbilisi, Georgia

Received 22 August 2012 / Accepted 14 November 2012

ABSTRACT

Context. Ion-neutral collisions may lead to the damping of Alfvén waves in chromospheric and prominence plasmas. Neutral helium atoms enhance the damping in certain temperature intervals, where the ratio of neutral helium and neutral hydrogen atoms is increased. Therefore, the height dependence of the ionization degrees of hydrogen and helium may influence the damping rate of Alfvén waves.
Aims. We aim to study the effect of neutral helium on the damping of Alfvén waves in stratified, partially ionized plasma of the solar chromosphere.
Methods. We consider a magnetic flux tube, which is expanded up to 1000 km height and then becomes vertical owing to merging with neighboring tubes, and study the dynamics of linear torsional Alfvén waves in the presence of neutral hydrogen and neutral helium atoms. We start with a three-fluid description of plasma and subsequently derive single-fluid magnetohydrodynamic (MHD) equations for torsional Alfvén waves. Thin flux tube approximation allows us to obtain the dispersion relation of the waves in the lower part of tubes, while the spatial dependence of steady-state Alfvén waves is governed by a Bessel-type equation in the upper parts of the tubes.
Results. Consecutive derivation of single-fluid MHD equations results in a new Cowling diffusion coefficient in the presence of neutral helium, which is different from the previously used one. We find that shorter period (<5 s) torsional Alfvén waves damp quickly in the chromospheric network owing to ion-neutral collision. On the other hand, longer period (>5 s) waves do not reach the transition region because they become evanescent at lower heights in the network cores.
Conclusions. Propagation of torsional Alfvén waves through the chromosphere into the solar corona should be considered with caution: low-frequency waves are evanescent owing to the stratification, while high-frequency waves are damped by ion-neutral collisions.

Key words. Sun: atmosphere – Sun: oscillations

1. Introduction

Alfvén waves play an important role in the dynamics of the solar atmosphere. Photospheric motions may excite the waves, which then propagate upwards along the anchored magnetic field and transport the energy into upper layers, where they may deposit the energy back leading to the chromospheric/coronal heating and/or the acceleration of solar wind particles. The photospheric magnetic field is concentrated in flux tubes, which are very dynamic and may continuously change shape and/or merge because of granular motions. Nevertheless, in a crude representation useful for theoretical modeling, the magnetic field can be approximated as axis-symmetric tubes, therefore the excited pure Alfvén waves are axis-symmetric; i.e. they are torsional Alfvén waves. If considering a cylindrically symmetric flux tube, torsional waves correspond to the azimuthal wavenumber set to $m = 0$ in the standard notation. On the other hand, granular buffeting may excite transverse magnetohydrodynamic (MHD) kink waves in the tubes, which then can be transformed into linearly polarized Alfvén waves in the upper layer thanks to the expansion of tubes (Cranmer & van Ballegooijen 2005). The transverse oscillations have been observed with both imaging and spectroscopic observations (Kukhianidze et al. 2006; Zaqarashvili et al. 2007; De Pontieu et al. 2007, the interested reader may find a detailed review of oscillations in Zaqarashvili & Erdélyi 2009).

Torsional Alfvén waves do not lead to the displacement of magnetic tube axis, therefore they can only be observed with spectroscopic observations as a periodic variation in spectral line width (Zaqarashvili 2003). Observations of torsional Alfvén waves have been recently reported in chromospheric spectral lines (Jess et al. 2009; De Pontieu et al. 2012). Upward propagating undamped Alfvén waves can also be observed in the solar corona as an increase in nonthermal broadening of coronal spectral lines with height (Hassler et al. 1990).

The dynamics of Alfvén waves in the chromosphere/corona and their role in plasma heating have been studied quite well (Hollweg 1981, 1984; Copil et al. 2008; Antolin & Shibata 2010; Vasheghani Farahani et al. 2010, 2011; Morton et al. 2011). They can be excited by the vortex motion at the photospheric level (Fedun et al. 2011a). In the case of inhomogeneous plasma, Alfvén waves may also be excited by resonances with other wave modes (see, e.g., Soler et al. 2012). Torsional Alfvén waves can be used as supplementary tool for solar magnetoseismology

(Zaqarashvili & Murawski 2007; Verth et al. 2010; Fedun et al. 2011b).

In the solar chromosphere and prominences, plasma is only partially ionized, which leads to damping of Alfvén waves owing to collision between ions and neutral hydrogen atoms (De Pontieu et al. 2001; Khodachenko et al. 2004; Leake et al. 2005; Forteza et al. 2007; Soler et al. 2009; Carbonell et al. 2010; Singh & Krishan 2010). Upward propagating Alfvén waves may also drive spicules through ion-neutral collisions (Haerendel 1992; James & Erdélyi 2002; Erdélyi & James 2004).

Single-fluid MHD description is a good approximation for low-frequency waves, but it fails when the wave frequency approaches an ion-neutral collision frequency, and consequently the multi-fluid MHD description should be used. It was shown by Zaqarashvili et al. (2011a) that the damping rate is maximum for the waves those frequency is near an ion-neutral collision frequency; i.e., higher and lower frequency waves have less damping rates.

Besides the neutral hydrogen atoms, the solar plasma may contain significant amount of neutral helium atoms, which may enhance the damping of Alfvén waves. Soler et al. (2010) suggested that the neutral helium has no significant influence on the damping rate in the prominence cores with 8000 K temperature. On the other hand, Zaqarashvili et al. (2011b) showed that the neutral helium may significantly enhance the damping of Alfvén waves in the temperature interval of 10 000–40 000 K, where the ratio of neutral helium and neutral hydrogen atoms is increased. This means that the helium atoms can be important in upper chromosphere, spicules, and prominence-corona transition regions. The neutral helium effects in Zaqarashvili et al. (2011b) was calculated in a homogeneous medium with uniform magnetic field and ionization degree. On the other hand, the ion and neutral atom number densities, hence ionization degree, are significantly changed with height in the chromosphere, which may influence the damping of Alfvén waves due to ion-neutral collisions.

Stratification may significantly influence the dynamics of waves, leading to their reflection in the transition region, mutual transformation, and/or evanescence. It introduces a cut-off frequency for Alfvén waves in fully ionized plasma; i.e., waves with lower frequency than the cut-off value are evanescent in the solar atmosphere (Musielak et al. 1995; Murawski & Musielak 2010).

In this paper, we study the effects of stratification and neutral helium atoms on the propagation/damping of Alfvén waves in the solar chromosphere. We consider a magnetic flux tube, which is expanded up to 1000 km height and then becomes vertical owing to merging with neighboring tubes. Consequently, we consider torsional Alfvén waves, which are only purely incompressible waves in tubes.

2. Linear torsional Alfvén waves

We consider a vertical magnetic flux tube embedded in the stratified solar atmosphere. We use cylindrical coordinate system (r, θ, z) and suppose that the unperturbed magnetic field, $\boldsymbol{B}_0$, is untwisted i.e. $B_{0\theta} = 0$. Plasma consists in electrons, protons (H^+), singly ionized helium (He^+), neutral hydrogen (H), and neutral helium (He) atoms. We consider the Alfvén waves polarized in θ direction; i.e., the only non-zero components of the perturbations are v_θ and b_θ. Therefore, the waves are torsional Alfvén waves. We start with the three-fluid approach for partially ionized hydrogen-helium plasma, when one component is ion + electron gas and the other two components are neutral hydrogen and neutral helium gasses (Zaqarashvili et al. 2011b). Then, the linear Alfvén waves are governed by the following equations (magnetic diffusion due to ion-electron collision is neglected):

$$\frac{\partial}{\partial t}(rv_\theta) = \frac{\boldsymbol{B}_0\cdot\nabla}{4\pi\rho_{\rm i}}(rb_\theta) - \frac{\alpha_{\rm H}+\alpha_{\rm He}}{\rho_{\rm i}}(rv_\theta) + \frac{\alpha_{\rm H}}{\rho_{\rm i}}(rv_{\rm H\theta}) + \frac{\alpha_{\rm He}}{\rho_{\rm i}}(rv_{\rm He\theta}), \quad (1)$$

$$\frac{\partial}{\partial t}(rv_{\rm H\theta}) = \frac{\alpha_{\rm H}}{\rho_{H0}}(rv_\theta) - \frac{\alpha_{\rm H}+\alpha_{\rm HeH}}{\rho_{\rm H0}}(rv_{\rm H\theta}) + \frac{\alpha_{\rm HeH}}{\rho_{H0}}(rv_{\rm He\theta}), \quad (2)$$

$$\frac{\partial}{\partial t}(rv_{\rm He\theta}) = \frac{\alpha_{\rm He}}{\rho_{\rm He0}}(rv_\theta) - \frac{\alpha_{\rm He}+\alpha_{\rm HeH}}{\rho_{\rm He0}}(rv_{\rm He\theta}) + \frac{\alpha_{\rm HeH}}{\rho_{He0}}(rv_{\rm H\theta}), \quad (3)$$

$$\frac{\partial b_\theta}{\partial t} = r(\boldsymbol{B}_0\cdot\nabla)\left(\frac{v_\theta}{r}\right), \quad (4)$$

where v_θ ($v_{\rm H\theta}$, $v_{\rm He\theta}$) are the perturbations of ion (neutral hydrogen, neutral helium) velocity, b_θ is the perturbation of the magnetic field, and $\rho_{\rm i}$ ($\rho_{\rm H0}$, $\rho_{\rm He0}$) is the unperturbed ion (neutral hydrogen, neutral helium) density. Here we use the definitions

$$\alpha_{\rm H} = \alpha_{\rm H^+H} + \alpha_{\rm He^+H}, \;\; \alpha_{\rm He} = \alpha_{\rm H^+He} + \alpha_{\rm He^+He}, \quad (5)$$

where α denotes the coefficient of friction between different sorts of species. The collision between electrons and neutral atoms is also neglected since it has much less of an effect on the damping of MHD waves than the collision between ions and neutrals. In the present model the motions of torsional Alfvén waves are normal to the direction of gravity, so that gravity does not explicitly appear in the equations. The effect of gravity is indirectly present in the equations through the stratification of plasma density.

The coefficient of friction between ions and neutrals (in the case of same temperature) is calculated as (Braginskii 1965)

$$\alpha_{\rm in} = n_{\rm i} n_{\rm n} m_{\rm in} \sigma_{\rm in} \frac{4}{3}\sqrt{\frac{8kT}{\pi m_{\rm in}}}, \quad (6)$$

where T is the plasma temperature, $m_{\rm i}$ ($m_{\rm n}$) the ion (neutral atom) mass, $m_{\rm in} = m_{\rm i}m_{\rm n}/(m_{\rm i}+m_{\rm n})$ is reduced mass, $n_{\rm i}$ ($n_{\rm n}$) is the ion (neutral atom) number density, $\sigma_{\rm in} = \pi(r_{\rm i}+r_{\rm n})^2 \approx \pi r_{\rm n}^2$ is the ion-neutral collision cross section for direct, elastic collisions from Braginskii (1965) (mean atomic cross section is $\pi r_{\rm n}^2 = 8.7974\times10^{-17}$ cm^2), and $k = 1.38\times10^{-16}$ erg K^{-1} is the Boltzmann constant.

From here we adopt the single-fluid approximation. To justify whether or not the single-fluid approximation is valid in the solar atmosphere we estimate the ion-neutral collision frequency. Mean collision frequency between ions and neutrals can be calculated as (Zaqarashvili et al. 2011b)

$$\nu_{\rm in} = \alpha_{\rm in}\left(\frac{1}{m_{\rm i}n_{\rm i}} + \frac{1}{m_{\rm n}n_{\rm n}}\right). \quad (7)$$

The collision frequency is very high in the photosphere and decreases upwards. For example, The collision frequency between protons and neutral hydrogen can be estimated as 8.6×10^6 Hz, 6.2×10^3 Hz, and 24 Hz, at $z = 0$, $z = 900$ km, and $z = 1900$ km correspondingly. Ion and neutral atom number densities were taken from Fontenla et al. (1993, model-F). Therefore, the Alfvén waves with periods >1 s can be studied in the single-fluid approach.

To obtain the governing equations in the single-fluid approximation, we consider the total density

$$\rho = \rho_{\rm i} + \rho_{\rm H} + \rho_{\rm He} \quad (8)$$

and the velocity of center of mass

$$V_\theta = \frac{\rho_i v_\theta + \rho_H v_{H\theta} + \rho_{He} v_{He\theta}}{\rho_i + \rho_H + \rho_{He}}. \quad (9)$$

We also consider the relative velocity of ion and neutral hydrogen as $w_{H\theta} = v_\theta - v_{H\theta}$ and the relative velocity of ion and neutral helium as $w_{He\theta} = v_\theta - v_{He\theta}$. Then one may find that

$$v_\theta = V_\theta + \xi_H w_{H\theta} + \xi_{He} w_{He\theta}, \quad (10)$$

where $\xi_H = \rho_H/\rho$ and $\xi_{He} = \rho_{He}/\rho$.

Consecutive substraction of Eqs. (1) and (2), Eqs. (1) and (3), Eqs. (2) and (3) and neglecting the inertial terms for relative velocities lead to the equations

$$r w_{H\theta} = \left[\frac{\alpha_{He}}{\alpha}\xi_H + \frac{\alpha_{HeH}}{\alpha}(\xi_H + \xi_{He})\right]\frac{\boldsymbol{B}_0\cdot\nabla}{4\pi}(r b_\theta), \quad (11)$$

$$r w_{He} = \left[\frac{\alpha_H}{\alpha}\xi_{He} + \frac{\alpha_{HeH}}{\alpha}(\xi_H + \xi_{He})\right]\frac{\boldsymbol{B}_0\cdot\nabla}{4\pi}(r b_\theta), \quad (12)$$

where $\alpha = \alpha_H\alpha_{He} + \alpha_H\alpha_{HeH} + \alpha_{He}\alpha_{HeH}$. Neglecting the inertial terms is justified for waves whose frequency is less than the ion-neutral collision frequency. This is the key step in transforming the multi fluid equations into the single fluid description.

Then the sum of Eqs. (1)–(3) and use of Eqs. (4), (10)–(12) lead to the single-fluid equations

$$\frac{\partial}{\partial t}(r V_\theta) = \frac{\boldsymbol{B}_0\cdot\nabla}{4\pi\rho(z)}(r b_\theta), \quad (13)$$

$$\frac{\partial b_\theta}{\partial t} = r(\boldsymbol{B}_0\cdot\nabla)\left(\frac{V_\theta}{r}\right) + r(\boldsymbol{B}_0\cdot\nabla)\left[\frac{\eta_c(z)}{B_0^2}\frac{\boldsymbol{B}_0\cdot\nabla}{r^2}(r b_\theta)\right], \quad (14)$$

where

$$\eta_c = \frac{B_0^2}{4\pi}\frac{\alpha_{He}\xi_H^2 + \alpha_H\xi_{He}^2 + \alpha_{HeH}(\xi_H + \xi_{He})^2}{\alpha_H\alpha_{He} + \alpha_H\alpha_{HeH} + \alpha_{He}\alpha_{HeH}} \quad (15)$$

is the coefficient of Cowling diffusion. The first two terms in the nominator of Eq. (15) are due the frictions of neutral hydrogen and neutral helium separately with regard to ions, while the last term is the friction of neutral hydrogen+helium fluid with regards to ions. Therefore, the last term is important in weakly ionized plasmas, while the first two terms are important for a relatively high value for the ionization degree. Soler et al. (2010) used the following expression for Cowling diffusion in the presence of neutral helium

$$\eta_c = \frac{B_0^2}{4\pi}\frac{(\xi_H + \xi_{He})^2}{\alpha_H + \alpha_{He}}, \quad (16)$$

which can be obtained from our expression (Eq. (15)) when $\alpha_H, \alpha_{He} \ll \alpha_{HeH}$, i.e., when plasma is only weakly ionized. This is so because in their derivation Soler et al. (2010) considered that both neutral hydrogen and neutral helium have the same velocity. That is equivalent to takeing $\alpha_{HeH} \to \infty$. Therefore the present description is more general than that of Soler et al. (2010). The expression used by Soler et al. (2010) is only approximately valid for the photosphere and lower chromosphere, while the general expression Eq. (15) should be used in the upper chromosphere, spicules and prominences.

We next consider a new coordinate s, which represents a longitudinal coordinate along the unperturbed magnetic field, $\boldsymbol{B}_0$.

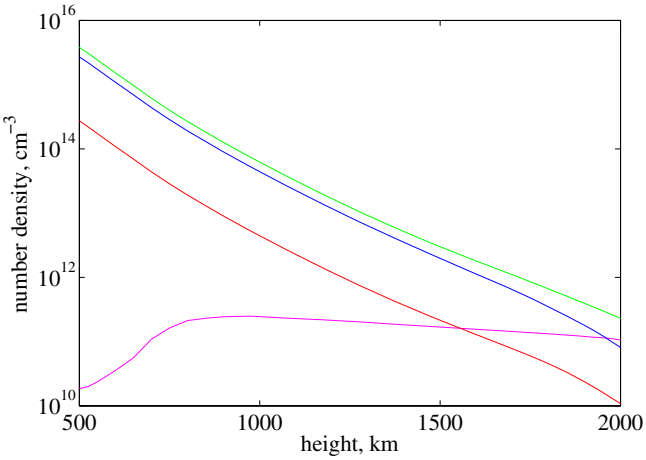

Fig. 1. Height dependence of atmospheric parameters according to FAL93-F model (Fontenla et al. 1993): magenta, red, and blue lines correspond to proton, neutral helium, and neutral hydrogen number densities, respectively. Green line is the total (proton + neutral hydrogen+neutral helium) number density.

Then Eqs. (13), (14) can be combined into the single equation in terms of this new coordinate, namely

$$\frac{\partial^2 U_\theta}{\partial t^2} = \frac{B_{0s}}{4\pi\rho r^2}\frac{\partial}{\partial s}\left[r^2 B_{0s}\frac{\partial U_\theta}{\partial s}\right] + \frac{B_{0s}}{4\pi\rho r^2}\frac{\partial}{\partial s}\left[r^2 B_{0s}\frac{\partial}{\partial s}\left(\frac{4\pi\rho\eta_c}{B_{0s}^2}\frac{\partial U_\theta}{\partial t}\right)\right], \quad (17)$$

where $U_\theta = V_\theta/r$. We note that r is a function of s. This equation is simplified near the axis of symmetry, where $B_{0s}(s)r^2(s) \approx$ const. (Hollweg 1981), which is the conservation of magnetic flux near the tube axis, where field lines are almost perpendicular to the tube's cross-section. Then this equation may be written as

$$\frac{\partial^2 U_\theta}{\partial t^2} = V_A^2(s)\frac{\partial^2}{\partial s^2}\left[\left(1 + \frac{\eta_c(s)}{V_A^2(s)}\frac{\partial}{\partial t}\right)U_\theta\right], \quad (18)$$

where

$$V_A = \frac{B_{0s}(s)}{\sqrt{4\pi\rho(s)}} \quad (19)$$

is the Alfvén speed.

Solar atmospheric parameters depend on the height owing to gravity. The plasma ionization degree is also a function of altitude because of the increase in temperature with height. The plasma is only weakly ionized in the photosphere/lower chromosphere. The increase in temperature with height leads to the ionization of hydrogen and helium atoms, which become almost fully ionized in the solar corona, so the transition occurs near the region of a sharp temperature rise.

Figure 1 shows the density of different species vs. height according to the FAL93-F model (Fontenla et al. 1993). This model includes the dependence of ionization degree on the heights for both hydrogen and helium. The neutral atom number densities are much higher than the ion number densities at the lower heights, but become comparable near ~1900 km, which corresponds to the temperature of about 10 000 K. It is seen that the neutral atoms are more stratified than protons between 500 and 2000 km heights: the neutral hydrogen, neutral helium, and total number densities have scale heights of about 180 km, while

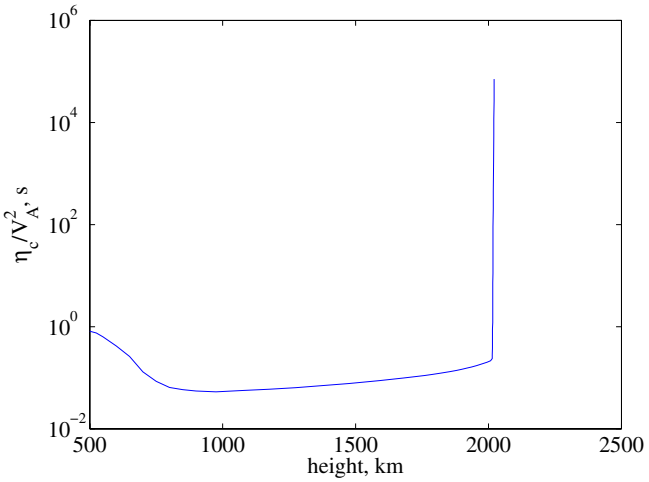

Fig. 2. Ratio of Cowling diffusion coefficient and Alfvén speed square, η_c/V_A^2, vs. height according to FAL93-F model (Fontenla et al. 1993).

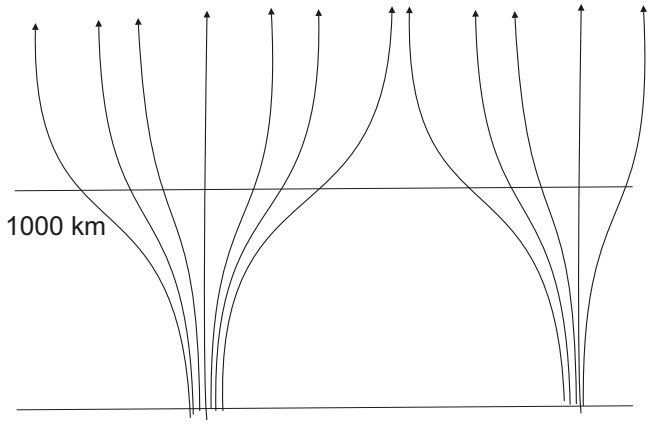

Fig. 3. Vertical magnetic flux tube model: below 1000 km the Alfvén speed is constant due to the thin flux tube approximation and above 1000 km height the Alfvén speed increases exponentially.

the scale height of protons is much greater. The total number density is similar to the neutral hydrogen number density until ~1500 km. Above this height they start to diverge due to the increase in ionization degree.

Fourier analysis of Eq. (18) with $\exp[-i\omega t]$, where ω is the wave frequency, gives the equation

$$V_A^2(s)\frac{\partial^2}{\partial s^2}\left[\left(1-i\frac{\omega\eta_c(s)}{V_A^2(s)}\right)U_\theta\right]+\omega^2 U_\theta=0, \quad (20)$$

which governs the spatial dependence of steady-state torsional Alfvén waves. The type of the equation depends on the dependence of V_A and η_c on s.

A very important parameter in Eq. (20) is the ratio η_c/V_A^2, which does not depend on the magnetic field structure with height because B_{0s}^2 is canceled. We plot the ratio vs. height according to the VAL93-F model in Fig. 2. It is clearly seen that the ratio is almost constant throughout the chromosphere and abruptly increases near the transition region. Therefore, to find analytical solutions to Eq. (20) we consider the ratio as a constant along s in the chromosphere

$$\frac{\eta_c(s)}{V_A^2(s)}\approx \text{const}. \quad (21)$$

From Fig. 2 we see that this approximation seems to be good in the upper part of the chromosphere, i.e., between 800−2000 km, while it may be not as accurate in the lower part of the chromosphere, i.e., in the interval between 500−800 km. Nevertheless, we use this approximation in the whole chromosphere for convenience.

Plasma β ($=8\pi p/B_{0s}^2$) is constant with height in the isothermal atmosphere in thin vertical magnetic flux tubes, when temperatures inside and outside the tubes are the same (Roberts 2004). In this case, the Alfvén speed is also constant with height, yielding $V_A(s) = V_{A0} = \text{const}$. The constancy of the Alfvén speed in thin tubes is caused by the compensation for density variation by the magnetic field strength variation with height. The thin flux tube approximation is valid up to 1000 km above the photosphere (Hasan et al. 2003; Cranmer & van Ballegooijen 2005). Above this height, the magnetic tubes are thick, and they probably merge with neighboring tubes to produce an almost vertical magnetic field (Fig. 3). Then, the Alfvén speed may vary with height owing to the decrease in density, while the magnetic field is constant. According to this model, we consider the vertical magnetic tube, which consists in two different parts: the lower part with constant Alfvén speed and the upper part with exponentially increasing Alfvén speed. Then we study the torsional Alfvén waves in the two parts of magnetic flux tube separately.

3. Lower chromosphere: thin flux tube approximation

In the lower part of the magnetic flux tube, the thin tube approximation is used, which yields $V_A(s) = \text{const}$. (see previous section). The thin tube approximation is still compatible with a magnetic flux tube expanding with height. The only restriction is that the wavelength remains much longer than the tube radius. This case was also studied by Soler et al. (2009) for the case of torsional Alfvén waves in prominence threads. The constancy of Alfvén speed means that the coefficient of Cowling diffusion is also constant. Then the coefficients of Eq. (20) do not depend on s, therefore Fourier analysis with $\exp[i(k_s s-\omega t)]$ gives the dispersion relation

$$\omega^2+i\eta_c k_s^2\omega-k_s^2V_A^2=0, \quad (22)$$

which has two complex solutions

$$\omega=\pm k_s V_A\sqrt{1-\frac{\eta_c^2k_s^2}{4V_A^2}}-i\frac{\eta_c k_s^2}{2}. \quad (23)$$

The dispersion relation and its solutions agree with Eqs. (33) and (34) of Soler et al. (2009). The real part of this expression gives the wave frequency, which shows that there is the cut-off wavenumber due to Cowling's diffusion, $k_s = 2V_A/\eta_c$. The cut-off wave number due to ion-neutral collision was found in different situations of the solar prominences (Forteza et al. 2007; Soler et al. 2009; Barcélo et al. 2011). It is the result of approximation when one transforms multifluid equations into the single-fluid MHD, and therefore it has no physical basis (Zaqarashvili et al. 2012).

On the other hand, the imaginary part of this expression gives the normalized damping rate as

$$|\tilde{\omega}_{\rm i}| = \left|\frac{\omega_{\rm i}}{k_{\rm s}V_{\rm A}}\right| = \frac{1}{2}\frac{k_{\rm s}V_{\rm A}}{\rho}\frac{\alpha_{\rm He}\rho_{\rm H}^2 + \alpha_{\rm H}\rho_{\rm He}^2 + \alpha_{\rm HeH}(\rho_{\rm H}+\rho_{\rm He})^2}{\alpha_{\rm H}\alpha_{\rm He} + \alpha_{\rm H}\alpha_{\rm HeH} + \alpha_{\rm He}\alpha_{\rm HeH}}, \tag{24}$$

where we have used the full expression of Cowling's coefficient, $\eta_{\rm c}$. The plasma is almost neutral in the low chromosphere, therefore $\alpha_{\rm HeH} \gg \alpha_{\rm H}, \alpha_{\rm He}$. This leads to the normalized damping rate

$$|\tilde{\omega}_{\rm i}| \approx \frac{1}{2}\frac{k_{\rm s}V_{\rm A}}{\rho}\left[\frac{(\rho_{\rm H}+\rho_{\rm He})^2}{\alpha_{\rm H}+\alpha_{\rm He}}\right]. \tag{25}$$

This expression was used by Soler et al. (2010) to calculate the effect of neutral helium in prominence cores.

On the other hand, when the number density of neutral atoms is much less than ion number density, then $\alpha_{\rm HeH} \ll \alpha_{\rm H}, \alpha_{\rm He}$ and the normalized damping rate is

$$|\tilde{\omega}_{\rm i}| \approx \frac{1}{2}\frac{k_{\rm s}V_{\rm A}}{\rho}\left[\frac{\rho_{\rm H}^2}{\alpha_{\rm H}} + \frac{\rho_{\rm He}^2}{\alpha_{\rm He}}\right]. \tag{26}$$

When ion number density is similar to the number density of neutral atoms (as in spicules or in prominence cores), then the general expression of damping rate (Eq. (24)) should be used. The expression Eq. (24) may significantly change the contribution of neutral helium atoms.

Figure 4 shows the normalized damping time ($T_{\rm d}/T_0 = 1/\tilde{\omega}_{\rm i}$) vs. the period of Alfvén waves ($T_0 = 2\pi/k_{\rm s}V_{\rm A}$) for three different areas: a) FAL93-A corresponding to faint cell center area; b) FAL93-F corresponding to bright area of chromospheric network; and c) prominence cores. We use the following parameters: a) $n_{\rm i} = 3.26 \times 10^{10}$ cm^{-3}, $n_{\rm H} = 3.01 \times 10^{13}$ cm^{-3}, $n_{\rm He} = 3.01 \times 10^{12}$ cm^{-3} taken from FAL93-A at 975 km height corresponding to ≈5480 K temperature; b) $n_{\rm i} = 2.49 \times 10^{11}$ cm^{-3}, $n_{\rm H} = 5.24 \times 10^{13}$ cm^{-3}, $n_{\rm He} = 5.26 \times 10^{12}$ cm^{-3} was taken from FAL93-F at 975 km height corresponding to 6180 K temperature; and c) $n_{\rm i} = 10^{10}$ cm^{-3}, $n_{\rm H} = 2 \times 10^{10}$ cm^{-3}, $n_{\rm He} = 2 \times 10^{9}$ cm^{-3} was taken for prominence cores corresponding to 8000 K temperature. It is clearly seen that the presence of neutral helium atoms significantly enhances the damping of Alfvén waves. It is also seen that the damping of torsional Alfvén waves is more efficient in the faint cell center area in the chromosphere and in prominence cores, where the waves are damped over a few wave periods. On the other hand, the damping of torsional Alfvén waves due to ion-neutral collision is inefficient in the bright chromospheric network center. The clear difference in damping in these two areas can be understood in terms of the ion-neutral collision frequency. In the absence of neutral helium atoms, Eq. (24) can be rewritten as (Zaqarashvili et al. 2011b)

$$|\tilde{\omega}_{\rm i}| \approx \frac{1}{2}\frac{k_{\rm s}V_{\rm A}}{\nu_{\rm iH}}\frac{\rho_{\rm H}}{\rho_{\rm i}}, \tag{27}$$

which clearly indicates that the normalized damping rate depends on the ratio of Alfvén frequency over ion-neutral hydrogen collision frequency ($\nu_{\rm iH}$) and the ratio of neutral and ion fluid densities. For $\rho_{\rm i} \ll \rho_{\rm H}$, which is the case at 975 km height, ion-neutral hydrogen collision frequency is proportional to neutral hydrogen density, $\nu_{\rm iH} \sim \rho_{\rm H}$. This means that the normalized damping rate is inversely proportional to ion number density, $\rho_{\rm i}$. The proton number density is almost ten times lower in the cell center than in the network center, which leads to almost ten times difference in damping (Fig. 4).

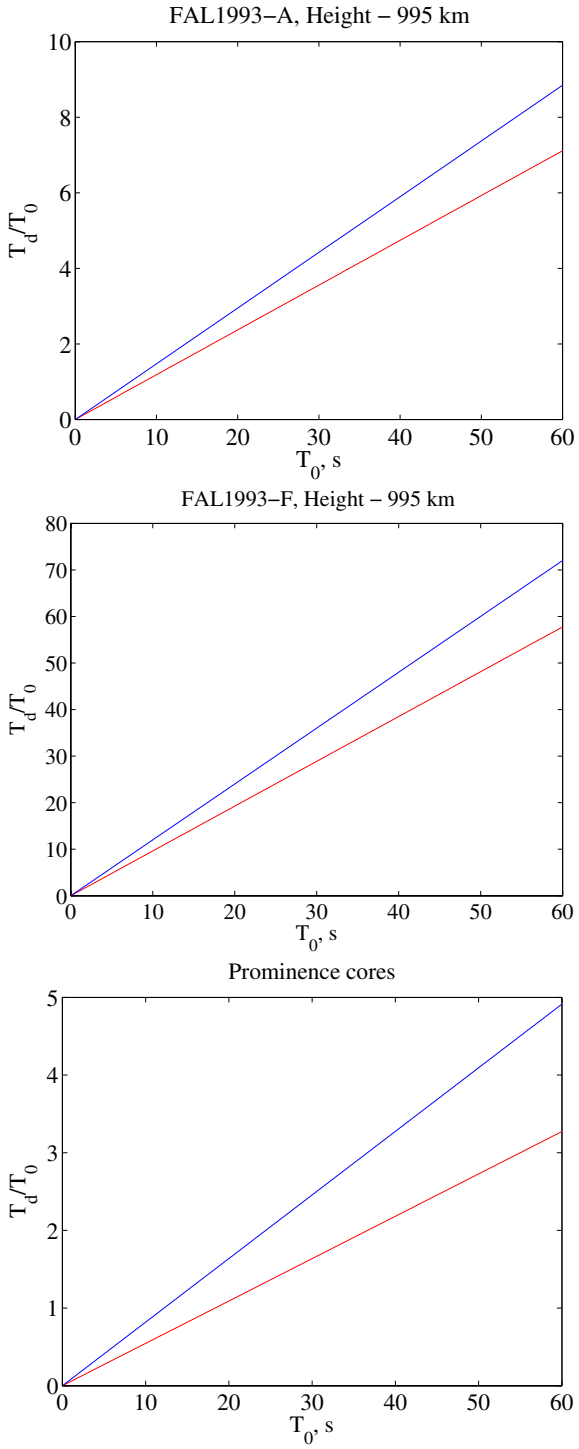

Fig. 4. Normalized damping time of torsional Alfvén waves ($T_{\rm d}/T_0$) vs. wave period (T_0) for three different situations from top to bottom: faint cell center area (FAL93-A), bright network (FAL93-F), and prominence core. The blue line indicates the wave damping due to collision of ions with neutral hydrogen atoms alone. The red line indicates the wave damping due to collision of ions with neutral hydrogen and neutral helium atoms.

In the first part of this section, we have studied the temporal damping of Alfvén waves, i.e., we set a real $k_{\rm s}$ and solved the dispersion relation to obtain the complex ω. In the following paragraphs, we study the spatial damping. This means that

the dispersion relation (Eq. (22)) is now solved for the complex wavenumber, k_s, assuming a fixed and real ω. The solution of the dispersion relation for the square of k_s is

$$k_s^2 = \frac{\omega^2}{V_A^2 - i\omega\eta_c}. \quad (28)$$

We use this expression to find the real and imaginary parts of k_s, assuming $k_s = k_r + ik_i$. After some algebraic manipulations we can obtain the expressions for k_r^2 and k_i, namely

$$k_r^2 = \frac{\omega^2 V_A^2}{2(V_A^4 + \omega^2\eta_c^2)} \pm \frac{\omega^2 V_A^2}{2(V_A^4 + \omega^2\eta_c^2)}\left(1 + \frac{\eta_c^2\omega^2}{V_A^4}\right)^{1/2}, \quad (29)$$

$$k_i = \frac{1}{k_r}\frac{\eta_c\omega^3}{2(V_A^4 + \omega^2\eta_c^2)}. \quad (30)$$

The expression of k_r is computed from Eq. (29) as $k_r = \pm\sqrt{k_r^2}$. The $\pm$ sign in front of the second term in the expression of k_r^2 leads to four possible values of k_r. The two values of k_r with + sign in the expression of k_r^2 correspond to propagating waves, namely

$$k_r = \pm\sqrt{\frac{\omega^2 V_A^2}{2(V_A^4 + \omega^2\eta_c^2)} + \frac{\omega^2 V_A^2}{2(V_A^4 + \omega^2\eta_c^2)}\left(1 + \frac{\eta_c^2\omega^2}{V_A^4}\right)^{1/2}} \quad (31)$$

where the $\pm$ sign in front of the square root refers to upward and downward waves.

To obtain more simplified analytical formulas we consider the case of weak damping; i.e., $\frac{\eta_c^2\omega^2}{V_A^4} \ll 1$. The expression of k_r for propagating waves becomes

$$k_r \approx \pm\sqrt{\frac{\omega^2 V_A^2}{V_A^4 + \omega^2\eta_c^2}\left(1 + \frac{\omega^2\eta_c^2}{4V_A^4}\right)} \approx \pm\frac{\omega}{V_A}\left(1 - \frac{3}{8}\frac{\omega^2\eta_c^2}{V_A^4}\right). \quad (32)$$

We now take the + sign corresponding to upward propagating waves and use this expression to compute the value of k_i in the limit $\frac{\eta_c^2\omega^2}{V_A^4} \ll 1$,

$$k_i \approx \frac{1}{2k_r}\frac{\eta_c\omega^3}{V_A^4} \approx \frac{\eta_c\omega^2}{2V_A^3}. \quad (33)$$

The corresponding normalized damping rate using the full expression of η_c is

$$\tilde{k}_i = \frac{k_i}{\omega/V_A} = \frac{1}{2}\frac{\omega}{\rho}\frac{\alpha_{He}\rho_H^2 + \alpha_H\rho_{He}^2 + \alpha_{HeH}(\rho_H + \rho_{He})^2}{\alpha_H\alpha_{He} + \alpha_H\alpha_{HeH} + \alpha_{He}\alpha_{HeH}}, \quad (34)$$

which is equivalent to Eq. (24) obtained for the temporal damping if we replace ω by $k_s V_A$. Therefore, both spatial and temporal damping rates of the Alfvén waves are equivalent.

On the other hand, the two values of k_r corresponding to the $-$ sign in the expression of k_r^2 (Eq. (29)) correspond to evanescent waves,

$$k_r = \pm\sqrt{\frac{\omega^2 V_A^2}{2(V_A^4 + \omega^2\eta_c^2)} - \frac{\omega^2 V_A^2}{2(V_A^4 + \omega^2\eta_c^2)}\left(1 + \frac{\eta_c^2\omega^2}{V_A^4}\right)^{1/2}}, \quad (35)$$

which for weak damping, i.e., $\frac{\eta_c^2\omega^2}{V_A^4} \ll 1$, becomes

$$k_r = \pm i\sqrt{\frac{\omega^4\eta_c^2}{4V_A^2(V_A^4 + \omega^2\eta_c^2)}}. \quad (36)$$

This corresponds to evanescent perturbations that do not propagate from the location of the excitation, so these solutions are not relevant for the present study.

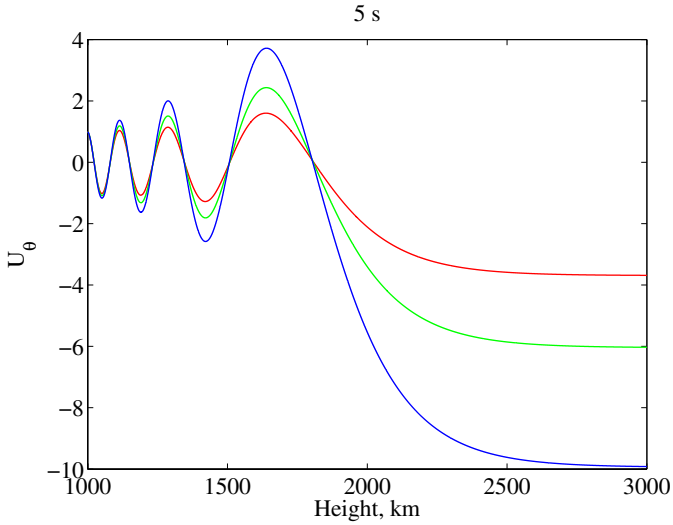

Fig. 5. Height dependence of steady-state, torsional Alfvén waves with periods of 5 s. Green line corresponds to $H_0^1(\zeta)$ and $H_0^2(\zeta)$ from Eq. (40) in fully ionized plasma. Blue and red lines correspond to $H_0^1(\zeta)$ and $H_0^2(\zeta)$, respectively, in partially ionized plasma.

4. Upper chromosphere: exponentially increasing Alfvén speed

In the upper part of magnetic flux tube, where the neighboring tubes are merged, we assume that the Alfvén speed is exponentially increasing (the ratio of Cowling diffusion coefficient and Alfvén speed square is assumed to be constant again),

$$V_A(s) = V_{A0}\exp\left(\frac{s}{2h}\right), \quad (37)$$

where h is the scale height and V_{A0} corresponds to the value of Alfvén speed at the height of 1000 km (i.e., $s = 0$ also corresponds to the height of 1000 km). In this case, Eq. (20) can be rewritten as

$$\frac{\partial^2 U_\theta}{\partial s^2} + \exp\left(-\frac{s}{h}\right)k_{s0}^2 U_\theta = 0, \quad (38)$$

where

$$k_{s0}^2 = \frac{\omega^2}{V_{A0}^2 - i\omega\eta_{c0}} \quad (39)$$

and η_{c0} is the value of Cowling diffusion at the height of 1000 km. The solution of this equation is

$$U_\theta = U_\theta(0)F_0(\zeta), \quad (40)$$

where F_0 is Bessel, modified Bessel or Hankel functions of zero order and

$$\zeta = 2hk_{s0}\exp\left[-\frac{s}{2h}\right].$$

Propagating waves are described by Hankel functions ($H_0^1(\zeta) = J_0(\zeta) + iY_0(\zeta)$, $H_0^2(\zeta) = J_0(\zeta) - iY_0(\zeta)$), and standing waves are described by Bessel functions ($J_0(\zeta)$). $H_0^1(\zeta)$ and $H_0^2(\zeta)$ functions have the same spatial dependence in the case of fully ionized plasma (Fig. 5). The upward and downward propagating waves can be distinguished by the sign of time-averaged Pointing flux (Hollweg 1984), which shows that $H_0^2(\zeta)$ is upward-propagating

and $H_0^1(\zeta)$ is downward-propagating waves. In the case of partially ionized plasma distinguishing between upward and downward propagating waves is complicated by the complex argument of Hankel functions (De Pontieu et al. 2001). However, it is still possible to distinguish them by a careful look into the height structure of waves (Fig. 5). $H_0^2(\zeta)$ has smaller amplitude at higher heights in partially ionized case compared to the fully ionized case, while $H_0^1(\zeta)$ has the stronger amplitude. This means that $H_0^2(\zeta)$ governs the wave, which damps at higher heights owing to ion-neutral collisions, therefore it governs the dynamics of upwardly propagating waves. On the same basis, $H_0^1(\zeta)$ governs the downwardly propagating waves. The standing waves, expressed by $J_0(\zeta)$, can be formed after superposition of upward- and downward-propagating waves.

A mathematical proof that the function H_0^2 corresponds to upward waves is obtained from the asymptotic expansion of the Hankel functions for large arguments (see, e.g., Stenuit et al. 1999). For large ζ, which eventually means small s, the dependence of Hankel functions on s can be written as

$$H_0^1(\zeta) \sim \exp(-\mathrm{i}|k_{s0}|s), \;\; H_0^2(\zeta) \sim \exp(\mathrm{i}|k_{s0}|s),$$

where k_{s0} is given in Eq. (39). These expansions clearly show that H_0^2 corresponds to upwardly propagating waves when the temporal dependence is $\exp[-\mathrm{i}\omega t]$. In the rest of the paper we only consider upwardly propagating waves. Only the real parts of $H_0^1(\zeta)$ and $H_0^2(\zeta)$, i.e., the part of the solution with the physical meaning, are shown in all plots.

Figure 6 shows the height dependence of upward propagating torsional Alfvén waves with different periods in the bright chromospheric network cores. At a 1000 km height we use the number densities from the FAL93-F model such as $n_\mathrm{i} = 3.22 \times 10^{11}$ cm^{-3}, $n_\mathrm{H} = 2.65 \times 10^{13}$ cm^{-3}, and $n_\mathrm{He} = 2.68 \times 10^{12}$ cm^{-3}. The plasma temperature is set as $T = 8000$ K and the Alfvén speed as $V_{A0} = 20$ km s^{-1}. It is seen that the behavior of longer period waves (>10 s) is not significantly affected by ion-neutral collisions: the height dependence is similar for fully ionized and partially ionized plasmas (upper panel). The shorter period waves display more significant dependence on ion-neutral collisions. For example, the torsional Alfvén waves with periods of 3 s are significantly damped in partially ionized plasma compared to the fully ionized case (lower panel). It is also seen that the presence of neutral helium enhances the damping of Alfvén waves compared to neutral hydrogen only. Figure 6 shows that the spatial dependence of waves is not oscillatory above particular heights; i.e., waves become evanescent. To study this phenomenon, we consider wave propagation in fully ionized plasma.

Figure 7 displays the velocity of torsional Alfvén waves vs. height for different wave periods. It is seen that torsional Alfvén waves with periods of 20 s become evanescent above a 1500 km height. Waves with 5 s periods become evanescent above a 1800 km height, but the waves with 1 s periods penetrate up to a 2600 km height. Therefore, the longer period waves (>5 s) do not reach transition region (2000 km height), but become evanescent at lower heights. This gravitational cut-off of Alfvén waves has been known for a long time (Musielak & Moore 1995). Recently, Murawski & Musielak (2010) have also shown that the linearly polarized Alfvén waves become evanescent above some heights in fully ionized plasma. Our result confirms their analyses.

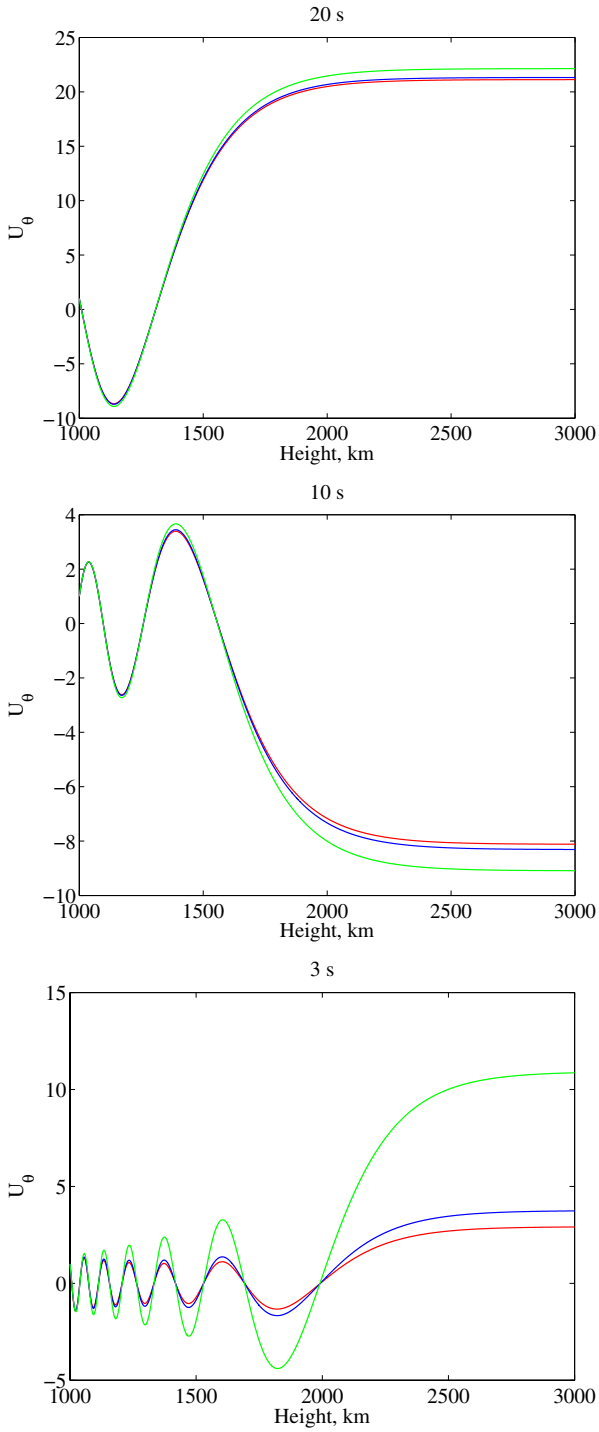

Fig. 6. Height dependence of steady-state, upward propagating torsional Alfvén waves with periods of 20 s (*upper panel*), 10 s (*middle panel*), and 3 s (*lower panel*). Green lines correspond to the fully ionized plasma, and blue (red) lines correspond to partially ionized plasma with neutral hydrogen atoms (neutral hydrogen + neutral helium atoms).

5. Discussion

Propagation of Alfvén waves in the chromosphere is very important for chromospheric/coronal heating because they may carry the photospheric energy into the upper layers. The magnetic field is concentrated in flux tubes at the photospheric level, therefore the torsional Alfvén waves can be generated by vortex motions (Fedun et al. 2011a). Observation of torsional Alfvén waves is possible through the periodic variation in spectral line width (Zaqarashvili 2003). Recently, Jess et al. (2009) have reported the observation of torsional Alfvén waves in the lower chromosphere. The energy flux carried by the waves was enough to heat

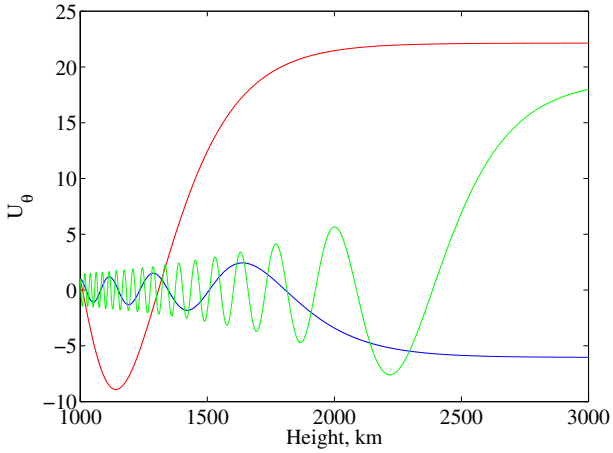

Fig. 7. Height dependence of steady-state, upward-propagating torsional Alfvén waves with periods of 20 s (red line), 5 s (blue line), and 1 s (green line) in fully ionized plasma.

the solar corona. Therefore, it is interesting to study whether the waves may penetrate the corona.

Here we study the torsional Alfvén waves in chromospheric magnetic flux tubes with partially ionized plasma taking neutral hydrogen and neutral helium atoms into account. We consider the stratification due to gravity, therefore the tubes are expanding with height. Hasan et al. (2003) showed that the magnetic flux tubes can be considered as thin up to a 1000 km height from the surface. Above this height, the neighboring magnetic flux tubes merge and the field lines are almost vertical. We use this model and split the magnetic tubes into two layers. We use the expanding thin flux tube approximation in the lower chromosphere below 1000 km. In the upper layer, above 1000 km we consider the magnetic field lines as vertical, so only medium density changes with height. We use the FAL93 model (Fontenla et al. 1993) for the dependence of ion, neutral hydrogen, and neutral helium number densities with height.

We start with a three-fluid MHD description of partially ionized plasma, where one component is electron-proton-singly ionized helium and the other two components are neutral hydrogen and neutral helium gasses. Then we proceed to the single-fluid description by standard procedures and neglect the inertial terms of ion-neutral hydrogen and ion-neutral helium relative velocities. We obtain the Cowling diffusion coefficient (Eq. (15)), which is different from the previously used one. Namely, the expression Eq. (15) contains additional terms (the first and second terms in nominator) that express the collision of ions with neutral hydrogen and neutral helium atoms separately. The previously used expression of the Cowling diffusion coefficient is valid in weakly ionized plasma, where the coupling between neutral atoms is stronger.

In the lower part of magnetic flux tube, where the thin tube approximations is used, the dispersion relation for the torsional Alfvén waves is obtained. The solution of the dispersion relation shows that the damping of Alfvén waves due to ion-neutral collision is significant in faint cell center areas at all frequencies, while only high-frequency waves are damped in the chromospheric network cores (Fig. 4). This means that torsional Alfvén waves may propagate without any problem up to 1000 km above the surface in chromospheric network cores. The effect of neutral helium atoms is significant in all cases, and it increases for lower frequency waves.

In the upper part of magnetic flux tube, the height dependence of torsional Alfvén wave velocity is governed by a Bessel-type equation, therefore the solutions are Bessel or Hankel functions with zero-order and complex arguments. We consider only upward propagating waves, which are expressed by Hankel functions, H_0^2. The solution of steady-state torsional Alfvén waves shows that the long-period waves are not affected by ion-neutral collisions. Only short-period waves (<5 s) are damped significantly (Fig. 6). The existence of neutral helium atoms enhances damping of the waves but not significantly. On the other hand, long-period waves show no oscillatory behavior above certain heights, so they become evanescent in the upper part of the chromosphere. This phenomenon is called gravitational cut-off (Musielak et al. 1995; Murawski & Musielak 2010). It is seen that only the waves with very short periods (∼1 s) may reach the transition region and corona in the case of fully ionized plasma (Fig. 7). This means that the low-frequency waves cannot reach the transition region due to the gravitational cut-off, but high-frequency waves are damped due to ion-neutral collision. Then the torsional Alfvén waves cannot reach the transition region at all. This is true near the axis of magnetic flux tubes, where our approximations are valid. However, it is possible that some wave tunneling exists there, and the evanescent tail of the waves can indeed reach the transition region and the corona. Owing to the change in the ambient conditions, the waves may propagate again in the corona. In the outer part of tubes, where magnetic field lines are more inclined, the problem of wave propagation along the chromosphere may not arise at all. This requires further detailed study.

On the other hand, Alfvén waves may easily penetrate the corona if they are excited in the higher part of the chromosphere (Hansen & Cally 2012). Long-period acoustic oscillations (p-modes) are evanescent in the lower atmosphere owing to the gravitational stratification; however, they may propagate with an angle about the vertical and may trigger Alfvén waves in the upper chromosphere through mode conversion (Zaqarashvili & Roberts 2006; Cally & Goossens 2008; Cally & Hansen 2011; Khomenko & Cally 2012). If low-frequency torsional Alfvén waves are excited above a 1000 km height, then our model also allows the propagation of the waves into the corona since the evanescent point can be shifted up above the transition region (Fig. 7).

Recently, Vranjes et al. (2008) have suggested that the energy flux of Alfvén waves excited in the photosphere is overestimated, and thus the Alfvén waves can hardly be excited in the photosphere (but see Tsap et al. 2011, for alternative point of view). This is indeed an interesting question that should be addressed adequately. One possible explanation is that Vranjes et al. (2008) considered the magnetic field strength of 100 G in the photosphere, which is too weak for flux tubes, where the magnetic field strength is of order kG. Therefore, it is possible that the Alfvén waves are excited only inside flux tubes, but not outside the tubes, where the magnetic field is relatively weak. This point needs further discussion.

Ion-neutral collisions are only important for short-period waves (<5 s). On the other hand, only long-period transverse oscillations (≥3 min) have so far been observed frequently in the solar atmosphere. However, some observations from ground based coronagraphs show the oscillations of spicule axes with periods of ≤1 min (Zaqarashvili et al. 2007; Zaqarashvili & Erdélyi 2009). Several reasons could explain the absence of high-frequency oscillations: not enough tempo-spatial resolution of observations, hard excitation in the photospheric level, quick damping in the lower atmosphere, etc. We hope that more

sophisticated observations will help us improve our knowledge about high-frequency oscillations in the future.

6. Conclusions

Propagation of torsional Alfvén waves along expanding vertical magnetic flux tubes in the partially ionized solar chromosphere was studied, the ion collisions with neutral hydrogen and neutral helium atoms taking into account. The waves propagate freely in the lower chromosphere up to 1000 km and may be damped by ion-neutral collisions. The new expression of the Cowling diffusion (and consequently damping rate) including the neutral helium was obtained (Eq. (15)). Neutral helium atoms may significantly enhance the damping of Alfvén waves. On the other hand, the long-period (>5 s) waves propagating near the tube axis become evanescent above some height in the upper chromosphere and do not reach the transition region, while the short-period waves (<5 s) are damped by ion-neutral collisions. As a result, the torsional Alfvén waves may not reach the transition region and the corona, unless some tunneling effects are considered. This means that the coronal heating by photospheric Alfvén waves should be considered with caution. At the same time, energy of the waves can be dissipated in the chromosphere, leading to the heating of ambient plasma.

Acknowledgements. The work was supported by the Austrian Fonds zur Förderung der wissenschaftlichen Forschung (project P21197-N16) and by the European FP7-PEOPLE-2010-IRSES-269299 project-SOLSPANET. R.S. acknowledges support from a Marie Curie Intra-European Fellowship within the European Commission 7th Framework Program (PIEF-GA-2010-274716). R.S. also acknowledges support from MINECO and FEDER funds through project AYA2011-22846 and from CAIB through the "Grups Competitius" scheme.

References

Antolin, P., & Shibata, K. 2010, ApJ, 712, 494
Barcélo, S., Carbonell, M., & Ballester, J. L. 2011, A&A, 525, A60
Braginskii, S. I. 1965, Rev. Plasma Phys., 1, 205
Cally, P. S., & Goossens, M. 2008, Sol. Phys., 251, 251
Cally, P. S., & Hansen, S. C. 2011, ApJ, 738, 119
Carbonell, M., Forteza, P., Oliver, R., & Ballester, J. L. 2010, A&A, 515, A80
Copil, P., Voitenko, Y., & Goossens, M. 2008, A&A, 478, 921
Cranmer, S. R., & van Ballegooijen, A. A. 2005, ApJ, 156, 265
De Pontieu, B., Martens, P. C. H., & Hudson, H. S. 2001, ApJ, 558, 859
De Pontieu, B., McIntosh, S. W., Carlsson, M., et al. 2007, Science, 318, 1574
De Pontieu, B., Carlsson, M., Rouppe van der Voort, L. H. M., et al. 2012, ApJ, 752, L12
Erdélyi, R., & James, S. P. 2004, A&A, 427, 1055
Fedun, V., Shelyag, S., Verth, G., Mathioudakis, M., & Erdélyi, R. 2011a, Ann. Geophys., 29, 1029
Fedun, V., Verth, G., Jess, D. B., & Erdélyi, R. 2011b, ApJ, 740, L46
Fontenla, J. M., Avrett, E. H., & Loeser, R. 1993, ApJ, 406, 319
Forteza, P., Oliver, R., Ballester, J. L., & Khodachenko, M. L. 2007, A&A, 461, 731
Haerendel, G. 1992, Nature, 360, 241
Hansen, S. C., & Cally, P. S. 2012, ApJ, 751, 31
Hasan, S. S., Kalkofen, W., van Ballegooijen, A. A., & Ulmschneider, P. 2003, ApJ, 585, 1138
Hassler, D. M., Rottman, G. J., Shoub, E. C., & Holzer, T. E. 1990, ApJ, 348, L77
Hollweg, J. V. 1981, Sol. Phys., 70, 25
Hollweg, J. V. 1984, ApJ, 277, 392
James, S. P., & Erdélyi, R. 2002, A&A, 393, L11
Jess, D. B., Mathioudakis, M., Erdïlyi, R., et al. 2009, Science, 323, 1582
Kukhianidze, V., Zaqarashvili, T. V., & Khutsishvili, E. 2006, A&A, 449, L35
Khodachenko M. L., Arber, T. D., Rucker, H. O., & Hanslmeier, A. 2004, A&A, 422, 1073
Khomenko, E., & Cally, P. S. 2012, ApJ, 746, 68
Leake, J. E., Arber, T. D., & Khodachenko, M. L. 2005, A&A, 442, 1091
Morton, R. J., Ruderman, M. S., & Erdélyi, R. 2011, A&A, 534, A27
Murawski, K., & Musielak, Z. E. 2010, A&A, 518, A37
Musielak, Z. E., & Moore, R. J. 1995, ApJ, 452, 434
Roberts, B. 2004, Proc. SOHO 13 – Waves, Oscillations and Small-Scale Transient Events in the Solar Atmosphere: A Joint View from SOHO and TRACE, ESA SP-547, 1
Singh, K. A. P., & Krishan, V. 2010, New Astron., 15, 119
Soler, R., Oliver, R., & Ballester, J. L. 2009, ApJ, 699, 1553
Soler, R., Oliver, R., & Ballester, J. L. 2010, A&A, 512, A28
Soler, R., Andries, J., & Goossens, M. 2012, A&A, 537, A84
Stenuit, H., Tirry, W. J., Keppens, R., & Goossens, M. 1999, A&A, 342, 863
Tsap, Y. T., Stepanov, A. V., & Kopylova, Y. G. 2011, Sol. Phys., 270, 205
Vasheghani Farahani, S., Nakariakov, V. M., & van Doorsselaere, T. 2010, A&A, 517, A29
Vasheghani Farahani, S., Nakariakov, V. M., van Doorsselaere, T., & Verwichte, E. 2011, A&A, 526, A80
Verth, G., Erdélyi, R., & Goossens, M. 2010, ApJ, 714, 1637
Vranjes, J., Poedts, S., Pandey, B. P., & de Pontieu, B. 2008, A&A, 478, 553
Zaqarashvili, T. V. 2003, A&A, 399, L15
Zaqarashvili, T. V., & Erdélyi, R. 2009, Space Sci. Rev., 149, 355
Zaqarashvili, T. V., & Murawski, K. 2007, A&A, 470, 353
Zaqarashvili, T. V., & Roberts, B. 2006, A&A, 452, 1053
Zaqarashvili, T. V., Khutsishvili, E., Kukhianidze, V., & Ramishvili, G. 2007, A&A, 474, 627
Zaqarashvili, T. V., Khodachenko, M. L., & Rucker H. O. 2011a, A&A, 529, A82
Zaqarashvili, T. V., Khodachenko, M. L., & Rucker H. O. 2011b, A&A, 534, A93
Zaqarashvili, T. V., Carbonell, M., Ballester, J. L., & Khodachenko, M. L. 2012, A&A, 544, A143